Journal of Power Sources 241 (2013) 136–145

Contents lists available at SciVerse ScienceDirect

Journal of Power Sources

journal homepage: www.elsevier.com/locate/jpowsour

The in-plane thermal conductivity and the contact resistance of the components of the membrane electrode assembly in proton exchange membrane fuel cells

N. Alhazmi*, M.S. Ismail, D.B. Ingham, K.J. Hughes, L. Ma, M. Pourkashanian

Centre for Computational Fluid Dynamics, Energy Technology Innovation Initiative, The University of Leeds, LS2 9JT, UK

HIGHLIGHTS

- The thermal conductivity of the membrane decreases when the temperature increases.
- The in-plane thermal conductivity of the GDL decreases as the temperature increases.
- The in-plane thermal conductivity of the GDL increases slightly with PTFE loading.
- The in-plane thermal conductivity of the GDL is higher in the samples which contain MPL.
- The in-plane thermal conductivity of the catalyst layer was found to be insensitive to the temperature and increases with Pt loading.

ARTICLE INFO

Article history:
Received 3 February 2013
Received in revised form
15 April 2013
Accepted 23 April 2013
Available online 29 April 2013

Keywords:
In-plane thermal conductivity
Gas diffusion layer
Micro porous layer
Catalyst layer
Membrane
Fuel cell

ABSTRACT

Understanding the thermal properties of the materials which are used in a proton exchange membrane fuel cell (PEM) is essential for the thermal management of a PEM fuel cell and consequently for improving its performance. In this paper, the parallel thermal conductance technique (PTC) has been employed to obtain the in-plane thermal conductivity and the contact resistance of several components of the membrane electrode assembly (MEA). In addition, the effects of temperature, polytetrafluoroethylene (PTFE) loading, micro porous layer (MPL) coating and the fibre direction on the in-plane thermal conductivity of the gas diffusion layer (GDL) have been investigated. The in-plane thermal conductivity of the GDL was found to decrease with increasing temperature and increase slightly with increasing PTFE loading and MPL coating. Further, the in-plane thermal conductivity of the membrane increased with higher amounts of water in the membrane. The in-plane thermal conductivity of the catalyst layer was found to be insensitive to the temperature and it increased with platinum loading.

1. Introduction

The proton exchange membrane (PEM) fuel cell has a promising role in the future energy production due to its ability to start-up fast, the low operating temperatures and the high power density. One of the keys for developing PEM fuel cell technology is thermal management. Furthermore, in order to understand the heat transfer through a PEM fuel cell, the thermal properties of the PEM fuel cell elements, such as the membrane electrode assembly (MEA), are required to be known [1,2]. Moreover, the thermal conductivity of the gas diffusion layer (GDL) is anisotropic, i.e. it is different in the in-plane and through-plane directions. Many researchers use a steady state method to measure the thermal conductivity of GDLs in the through-plane direction [3–5]. Khandelwal and Mench [6] measured the through-plane thermal conductivity of a dry Nafion membrane, GDL and the catalyst layers by using the steady state method. The thermal conductivity of the Toray GDL is obtained to be 1.8 ± 0.27 W m^{-1} K^{-1}.

Burheim et al. [7] considered the thickness of 3 different Toray GDLs as a function of the compression pressure and they determined the contact resistance between the GDL and the aluminium apparatus. The experimental setup is designed to measure the thickness of the sample at different compression pressures. The through-plane thermal conductivity of dry and wet GDLs are reported to be 0.15 and 1.6 W m^{-1} K^{-1}, respectively.

Teertstra et al. [8] measured the in-plane thermal conductivity of a GDL at a mean temperature of 70 °C. The maximum thermal conductivity for Toray paper with 30% PTFE loading is found to be

* Corresponding author. Tel.: +44 113 343 5113; fax: +44 113 246 7310.
E-mail addresses: pm09neah@leeds.ac.uk, pm09neah@hotmail.com (N. Alhazmi).

0378-7753/$ – see front matter © 2013 Elsevier B.V. All rights reserved.
http://dx.doi.org/10.1016/j.jpowsour.2013.04.100

15.1 W m^{-1} K^{-1}. However, they did not calculate the contact resistance and the effects of the mean temperature have not been taken into account.

Sadeghi et al. [9] developed a test bed to measure the in-plane thermal conductivity of a GDL as a function of the PTFE loading. They found that the thermal conductivity of a stack of Toray papers is approximately constant with PTFE loading and it is about 17.5 W m^{-1} K^{-1} at a mean temperature of 65 °C. Furthermore, they assumed that the contact resistance between the GDL layers is negligible. However, the effect of the temperature on the in-plane thermal conductivity of the MEA is not taken into account.

Karimi et al. [10] measured the through-plane thermal conductivity of a GDL as a function of the compression load at a mean temperature of 70 °C. The through-plane thermal conductivity of untreated GDL is found to be in the range of 0.26–0.7 W m^{-1} K^{-1} at 0.7 and 13.8 bar, respectively. The thermal contact resistance between the GDL and the holder surface, which was made of iron, is 0.24 m^2 K W^{-1} at 0.7 bar and 6×10^{-5} m^2 K W^{-1} at 13.8 bar.

In the present study, the parallel thermal conductance (PTC) technique, which developed by Zawilski et al. [11] to measure the in-plane thermal conductivity of single carbon fibres, was employed to measure the in-plane thermal conductivity of several components of MEA at different operating temperatures. The thermal conductivities measured by the PTC were compared with those measured by the conventional steady state method. Furthermore, the effects of water content and temperature on the thermal conductivity of the membrane, and the effects of PTFE loading, fibre direction and micro porous layer coating on the in-plane thermal conductivity of GDL were investigated. The effect of platinum loading on the thermal conductivity of the catalyst layer was accurately investigated. These measurements provide a database for the in-plane thermal conductivity of a membrane, GDL and the catalyst layer required to accurately determine the temperature distribution within the MEA.

2. Materials and procedure

2.1. Test apparatus

An experimental apparatus was developed to measure the in-plane thermal conductivity of the MEA and is shown in Fig. 1. This apparatus consisted of two parts. The first part was fixed and called the hot plate since it was electrically heated. The second part was the cold plate and was adjustable. This enables one to measure the thermal resistance of various lengths of the sample so that the thermal contact resistance can be determined. The PTC technique was developed to accurately measure the thermal conductivity of the GDL and the MEA in a PEM fuel cell by measuring at steady state

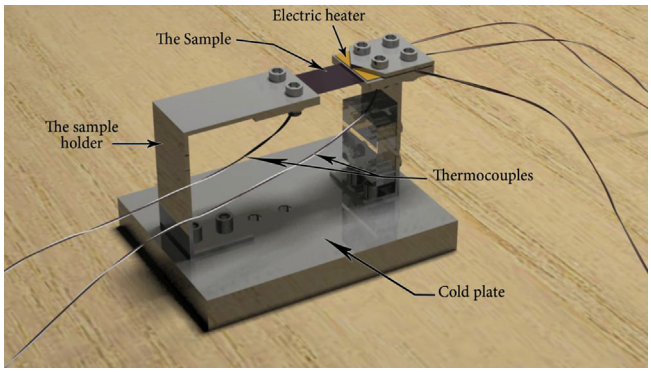

Fig. 1. Configuration of the sample holder and the experimental setup to measure the in-plane thermal conductivity of the MEA components.

Table 1
Manufacturers' specifications for the tested GDLs.

GDL	Thickness (μm)	PTFE loading (wt.%)
10AA	390	0
10BA	400	5
10CA	400	10
10DA	400	20
10EA	374	30
10BC	415	23[a]
10BE	367	50[a]

[a] PTFE loading in the MPL (wt.%).

the temperature drop and the voltage and current of the electric heater, from which the thermal conductivity of the sample was calculated based on the thermal resistance. This method is more accurate and more flexible than the conventional steady state method for measuring the thermal conductivity of very small samples because there is no dependence on the stress which may affect the measurement of the thermal conductivity, or even change the material properties with the compression pressure [12]. The conventional steady state method requires that the sample should be strong enough to sustain the thermal stress during the measurement.

Silicon rubber electric heaters (SRH-029) are attached to the upper end of the sample holder between the sample and the low thermal conductivity material. The hot plate temperature was about 100–120 °C. Since this assisted in providing a suitable power resolution and the temperature was in the same range that occurs in the operating conditions of PEM fuel cells. The sample holder was made of aluminium, which has a high thermal conductivity. A low thermal conductivity material was attached to the heat flow path between the heat source and the heat sink in order to ensure that the magnitude of the sample's thermal conductivity was at least one-tenth of the thermal conductance of the sample holder. The temperatures at the sides of the sample were measured using two thermocouples (PFA® T-Type). All readings; temperature, pressure, current and voltage were controlled and/or monitored via a LabVIEW application.

2.2. Experimental conditions

The in-plane thermal conductivity was measured for five GDL samples. The samples were provided by the SGL Technologies Gm bH, Germany. The thicknesses of these samples and their PTFE loading are listed in Table 1.

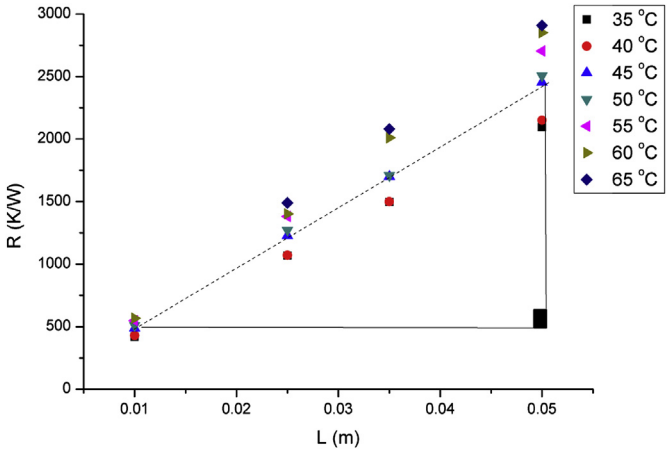

Fig. 2. Measured thermal resistances of the membrane as a function of the temperature by the conventional steady state technique.

Table 2
The thermal conductivity of the membrane as a function of the temperature by the conventional steady state technique.

The thermal conductivity (W m^{-1} K^{-1})						
35 °C	40 °C	45 °C	50 °C	55 °C	60 °C	65 °C
0.188 ± 0.015	0.183 ± 0.015	0.160 ± 0.013	0.158 ± 0.013	0.145 ± 0.012	0.138 ± 0.011	0.135 ± 0.011

The effect of the temperature on the in-plane thermal conductivity was investigated in the temperature range 35 °C–65 °C for the samples investigated in this study and all the measurements were made in a vacuum in order to eliminate convection and therefore minimise the heat transfer from the GDL to the surroundings. Therefore, neglecting radiation, the heat flow from the hot plate to the cold plate can be assumed to be one-directional through the sample via conduction.

The in-plane thermal conductivity of the GDLs investigated was evaluated in two orthogonal directions, namely when the orientation of most fibres was (i) parallel and (ii) normal to the heat flux. Furthermore, the effect of the PTFE loading on the in-plane thermal conductivity of the GDL was determined for five different samples (0, 5, 10, 20, and 30 wt.% PTFE loadings) and the orientation of the fibres was parallel to the heat flux. The effect of the micro porous layer (MPL) on the in-plane thermal conductivity of the GDL was determined for two different samples, namely 10BC and 10BE, and the thermal conductivity of them was compared with the main material 10BA without a micro porous layer.

The thermal conductivity of the membrane was determined for a Nafion® membrane using Nafion® 115 (Du Pont, USA), which is about 127 μm in thickness, and in the temperature range from 35 °C to 65 °C, which is most likely the mean temperature inside the PEM fuel cells.

The effect of Pt loading in the in-plane thermal conductivities of the catalyst layer was investigated for three samples with different platinum loading, namely 0.41, 0.45 and 0.51 mg cm^{-2}, which are within the realistic range available for the catalyst loading in PEM fuel cells.

2.3. Methodology

The thermal resistance of the holder without the sample, R_0, is measured as follows [13]:

$$R_0 = \frac{\Delta T}{IV} \tag{1}$$

where ΔT is the temperature drop across the holder, V is the voltage applied to the heater in the circuit, and I is the current applied to the heater.

In the second stage, the GDL sample is attached to the circuit and again the thermal resistance is calculated for the circuit with the sample. Subsequently, the total thermal resistance after attaching the sample is determined as follows:

$$R = \frac{\Delta T}{IV} \tag{2}$$

where R is the thermal resistance to the sample and the holder.

Finally, by subtracting the thermal resistance of the holder from the total thermal resistance, the thermal resistance of the sample is determined as follows:

$$\frac{1}{R_s} = \frac{1}{R} - \frac{1}{R_0} \tag{3}$$

where R_s is the thermal resistance of the sample [13].

By including the sample dimensions, the length and the cross-sectional area, the thermal conductivity of the sample is calculated as follows:

$$R_s = \frac{L}{kA} \tag{4}$$

where k is the thermal conductivity of the sample, L is the length of the sample and A is the cross-sectional area of the sample [13].

2.4. Uncertainty analysis

The uncertainty in the thermal conductivity measurements may be calculated based on the combined uncertainty in the power measurements [14]. The maximum uncertainty comes from the temperature measurements and it was about 0.5 °C for T-type thermocouples. The uncertainty in the measurements is calculated as follows:

$$\frac{\delta k}{k} = \sqrt{\left(\frac{\delta T_c}{T_c}\right)^2 + \left(\frac{\delta I}{I}\right)^2 + \left(\frac{\delta V}{V}\right)^2 + \left(\frac{\delta T_h}{T_h}\right)^2 + \left(\frac{\delta L}{L}\right)^2 + \left(\frac{\delta A}{A}\right)^2} \tag{5}$$

This value is calculated and reported for every measurement. It is important to note that the uncertainty in the measurements was not more than 6% for all the measurements performed in this investigation.

3. Results and discussions

3.1. Effect of the temperature on the in-plane thermal conductivity of the membrane

The thermal conductivity was obtained for dry Nafion® 115 membrane over a range of temperatures 35–65 °C. The thermal

Table 3
The thermal conductivity of the membrane as a function of the temperature by the parallel thermal conductance.

L (m)	The thermal conductivity (W m^{-1} K^{-1})						
	35 °C	40 °C	45 °C	50 °C	55 °C	60 °C	65 °C
0.01	0.187 ± 0.015	0.183 ± 0.015	0.161 ± 0.013	0.158 ± 0.012	0.144 ± 0.011	0.138 ± 0.011	0.134 ± 0.011
0.025	0.186 ± 0.015	0.184 ± 0.015	0.160 ± 0.013	0.158 ± 0.013	0.145 ± 0.011	0.139 ± 0.011	0.135 ± 0.011
0.035	0.188 ± 0.015	0.184 ± 0.015	0.160 ± 0.013	0.157 ± 0.013	0.144 ± 0.011	0.139 ± 0.011	0.135 ± 0.011
0.05	0.187 ± 0.015	0.183 ± 0.015	0.160 ± 0.013	0.157 ± 0.012	0.145 ± 0.012	0.138 ± 0.011	0.135 ± 0.011

conductivity is calculated from the slope of the curve for the thermal resistance versus the membrane length in the steady state thermal conductivity technique, see Fig. 2, as follow:

$$k = \frac{1}{\text{slope}} \times \frac{1}{A} \tag{6}$$

The thermal conductivities of the membrane which were calculated using the conventional steady state technique are listed in Table 2.

However, the thermal conductivity may be calculated directly from the thermal resistance in the parallel thermal conductance technique because the thermal contact resistances have been eliminated through the manipulation shown in Section 2.3.

$$k = \frac{L}{R_s A} \tag{7}$$

These thermal conductivities of the membrane as a function of the temperature, calculated by the parallel thermal conductance technique, are listed in Table 3.

It is clear that the thermal conductivities of the membrane calculated by both methods are in good agreement. However, by using the method of parallel thermal conductance, the thermal conductivity could be calculated immediately from one measurement of the thermal resistance. Therefore, the parallel thermal resistance could be used to measure the thermal resistance of a thin film accurately and in a short time.

As it can be seen in Fig. 3, the thermal conductivity of the membrane was 0.188 ± 0.015 W m^{-1} K^{-1} when the temperature was 35 °C, and as the temperature increases the thermal conductivity of the membrane slowly decreases. The thermal conductivity of the membrane at the maximum reported temperature, i.e. 65 °C, was 0.135 ± 0.011 W m^{-1} K^{-1}. This decrease with increasing temperature is due to the decrease in the phonon mean free path for the material of the Nafion® membranes [15]. It should be noted that these results are in good agreement with the reported thermal conductivities of the Nafion® by Kandelwal and Mench [6], see Fig. 3.

Typically, the membrane is humidified inside the fuel cell. However, it is difficult to measure the thermal conductivity of the humidified membrane because the heat generated in the apparatus used to measure the thermal conductivity will dry out the membrane. In addition, the measurement of the thermal conductivity of the membrane is performed under vacuum conditions and this will also make the membrane dry out from the original water content. Therefore, the effect of water on the thermal conductivity of the membrane was theoretically estimated based on the assumption that the wet membrane is a mixture of water and membrane material. The effective thermal conductivity of the wet membrane can then be calculated by averaging the thermal conductivity of the water, the air and the membrane to their volume fractions [16,17]:

$$k_{\text{eff}} = k_{\text{water}}\nu_{\text{water}} + k_{\text{air}}\nu_{\text{air}} + k_{\text{mem}}\nu_{\text{mem}} \tag{8}$$

where k_{water}, k_{air} and k_{mem} are the thermal conductivities of the water, air and membrane, respectively. ν_{water}, ν_{air} and ν_{mem} are the volume fractions of the water, air and membrane, respectively.

The volume fractions of water and membrane are calculated considering (i) the linear expansion of membrane when it is soaked with water and the extrapolated of these values at different temperatures, as listed in Table 4, and (ii) the porosity of the membrane, which is reported to be 0.28 [18,19].

However, it should be noted that the linear expansion of the membrane reported above is most likely to be limited inside the fuel cells and this is due to the presence of the ribs and the sealing gaskets in the fuel cells. Therefore, the thermal conductivity values of the wet membrane reported in Fig. 4 were the maximum possible ones inside the fuel cell.

It was observed that the thermal conductivity of the membrane significantly increases as it becomes wetter. This is due to the fact that the thermal conductivity of the water (k_{water} = 0.66 W m^{-1} K^{-1}) is more than the thermal conductivity of the membrane (k_{mem} = 0.18 W m^{-1} K^{-1}). It is also noteworthy that the thermal conductivity of water increases with increasing

Table 4
The physical properties of the fully-humidified Nafion® membrane [20].

Property	23 °C	100 °C
Thickness expansion (%)	10	14
Linear expansion (%)	10	15

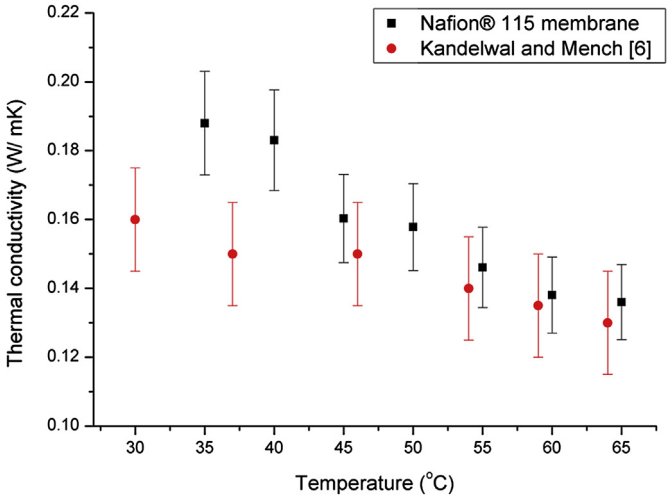

Fig. 3. Measured thermal conductivities of the membrane as a function of the temperature, including the experimental error bars.

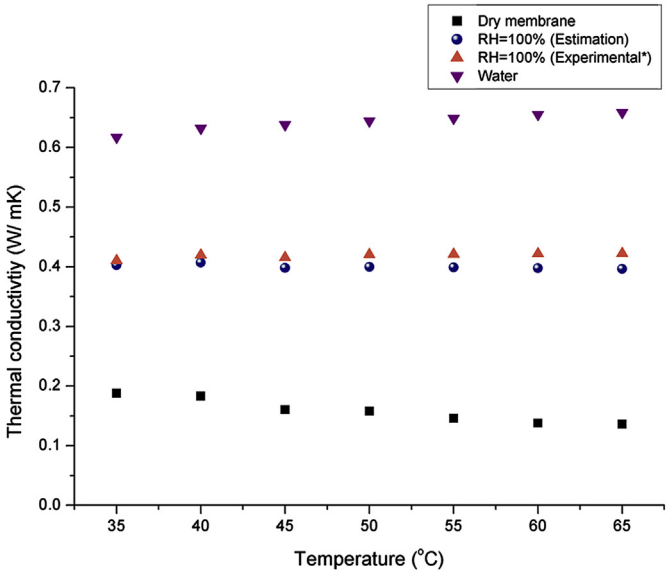

Fig. 4. Estimated thermal conductivity of dry and fully-humidified Nafion® membrane as a function of the temperature. *The experimental estimation of the volume fraction of the water.

the temperature [21]. Furthermore, the volume fraction of the water was measured experimentally by weighing a piece of membrane before and after being soaked with water. The difference in weight was assumed to be due to the addition of liquid water and subsequently converted to a volume fraction for water. As can be seen from Fig. 4, the thermal conductivity of the wet membrane that has been calculated based on the experimental estimation of the volume fraction of the water was in good agreement with that obtained based on the reported values for the linear expansion and porosity of the membrane. The dry membrane results give the lower bound for the thermal conductivity of the membrane, and the results of the membrane with 100% RH give the upper bound for the thermal conductivity of the membrane. In conclusion, Equation (8) should give a good estimate of the range of possible values for the thermal conductivity of a membrane within a fuel cell.

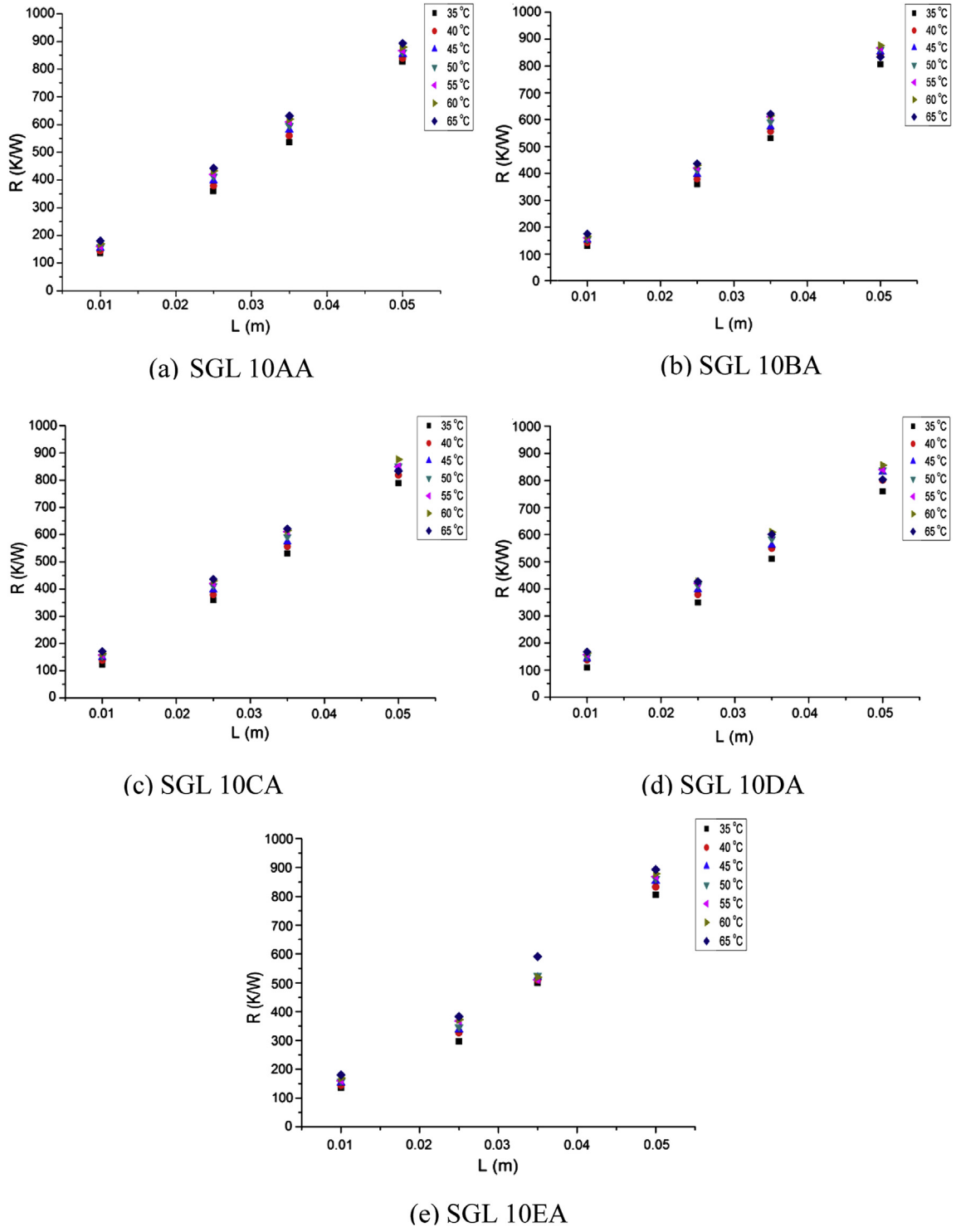

Fig. 5. Measured thermal resistances of the GDLs as a function of the temperature for (a) SGL 10AA, (b) SGL 10BA, (c) SGL 10CA, (d) SGL 10DA, and (e) SGL 10EA.

3.2. Effect of the temperature on the in-plane thermal conductivity of the GDL

Fig. 5 shows the thermal resistances of the GDLs as a function of the sample length for various temperatures. It was observed that the thermal resistance of the GDL increased as the temperature increases at normal operating temperatures that occur inside a PEM fuel cell. This is due to the presence of the binder whose thermal conductivities decrease with increasing temperature [22]. It was difficult to compare the in-plane thermal conductivity of the SGL GDL with that reported in the literature because they did not use the same type of GDL. However, the effect of temperature on the in-plane thermal conductivity of the GDL reported in this paper was in line with that reported by Zamel et al. [23].

3.3. Effect of the fibre direction on the in-plane thermal conductivity of the GDL

Due to the fibrous nature of the material used in GDLs, the thermal conductivity of the GDL is normally anisotropic. In order to illustrate this phenomenon, the thermal conductivity of 10AA which is cut in two perpendicular directions, namely where the fibres are parallel and normal to the heat flux were investigated. As mentioned in Section 2.2, the measurements were made for two sets of samples. The orientation of the fibres was parallel to heat flux in the first set and normal to heat flux in the second set. The thermal conductivity was found to be rather sensitive to the fibre direction, as shown in Fig. 6.

The in-plane thermal conductivity of the GDL was higher when the fibre orientation was parallel to the heat flux because the heat is transported more easily along the fibres than perpendicular to the fibres. The in-plane thermal conductivity of the SGL 10AA was determined to be 12.67 ± 0.17 and 11.9 ± 0.16 W m^{-1} K^{-1} at a mean temperature of 35 °C when the orientation of the fibre is parallel to the heat flux and normal to the heat flux, respectively. A similar ordering of thermal conductivities as a function of orientation were found for all the GDL samples under investigation.

3.4. Effect of the PTFE on the in-plane thermal conductivity of the GDLs

Polytetrafluoroethylene (PTFE) is a high molecular-weight fluorocarbon polymer which is usually known as Teflon. PTFE is a white solid thermoplastic at room temperature with a density of about 2.2 g cm^{-3}. The PTFE melts at a temperature of 327 °C and it is an insulating material with a thermal conductivity of approximately 0.25 W m^{-1} K^{-1} [24].

For fuel cells applications, the gas diffusion layers are usually treated with PTFE because of its hydrophobic properties. Therefore it minimises wetting of the GDL fibres during fuel cell operation, and hence minimises problems of blocking gas transport. The SGL samples which have been investigated in this paper have various PTFE loadings and the thicknesses of these samples are approximately 400 μm, as listed previously in Table 1.

The thermal conductivity of carbon is more than two orders of magnitude higher than that of the thermal conductivity of the PTFE. Therefore, the PTFE insulates the carbon fibres from each other. This will decrease the through-plane thermal conductivity of the gas diffusion layers since the heat transfer is from fibre to fibre in the through-plane direction. However, the contact resistance does not play a significant role in the through-plane direction as the fibres are under compression and the fibres will always be in contact.

On the other hand, most of the heat is transferred along the fibres in the in-plane direction and adding the PTFE decreases the contact resistance between the fibres and this increases the thermal conductivity in the in-plane direction and these effect was in a manner similar to that reported by Sadeghi et al. [9]. The measurements made that illustrate this are shown in Fig. 7. Furthermore, the temperature gradient decreases as the PTFE loading increases. Moreover, the contact resistance between the fibres reduces, which increases the thermal conductivity of the GDL. The overall thermal conductivity of the GDL increases as the PTFE loading increases and replaces the air, which has a thermal conductivity of ($k_{air} = 0.02$ W m^{-1} K^{-1}) [25], while the PTFE has a higher thermal conductivity ($k_{PTFE} = 0.25$ W m^{-1} K^{-1}) [24].

3.5. Effect of the MPL on the in-plane thermal conductivity of the GDL

The micro porous layer in the gas diffusion layer consists of a mix of hydrophobic agents with a layer of black powder carbon nanoparticles. This layer is added to the fuel cell between the gas diffusion layer and the catalyst layer in order to enhance the

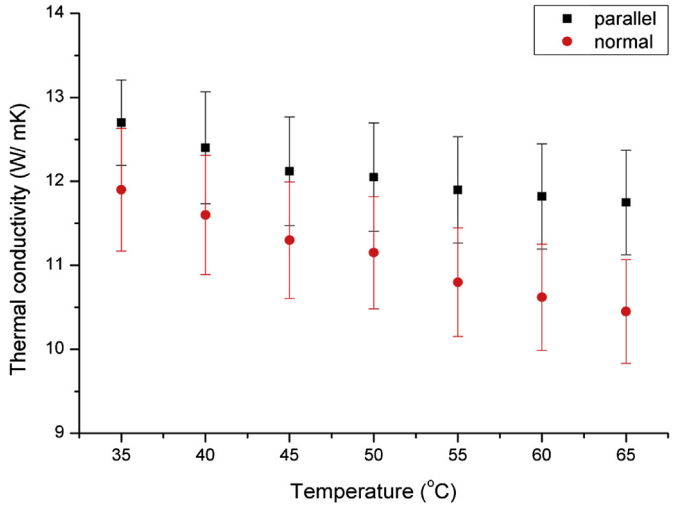

Fig. 6. Thermal conductivity of the 10AA GDL measured in two orthogonal in-plane directions, along with the experimental error bars.

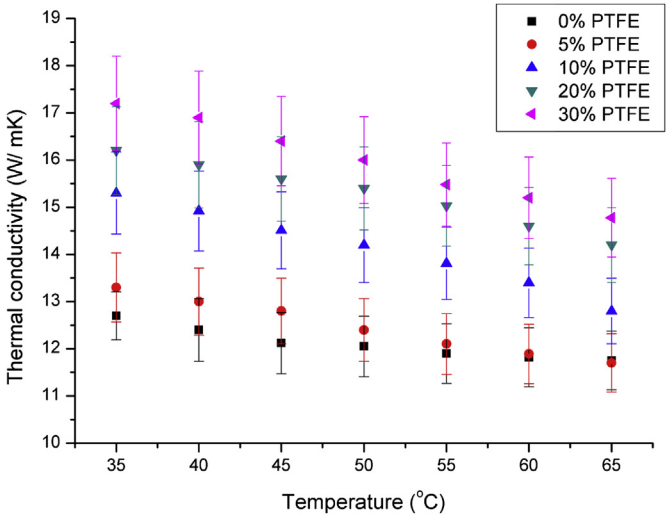

Fig. 7. Measured thermal conductivities of PTFE-treated GDLs as a function of the temperature, including the experimental error bars.

water management and to decrease the contact resistance between the gas diffusion layer and the catalyst layer [25].

The thermal contact resistance of the GDL samples decreases when the MPL is added to the GDL. This is not surprising as one of the main aims of adding MPL to the GDL in the fuel cell is to improve the contact between the GDL and the catalyst layer, as can be seen in Fig. 8.

A Philips XL30E5EM scanning electron microscope (SEM) has been used to image the surface of the GDL, as shown in Fig. 9. The sample which has the highest porosity and the largest pores was the 10 BA which was without an MPL. In addition, it is clear from the SEM images that the samples which have an MPL have a lower porosity than the samples without the MPL. However, it should be stressed that the mercury porosimetry and the method of stand porosimetry (MSP) are required to measure the three-dimensional microstructure of the pores and to obtain a full view for the pore sizes [26].

Furthermore, it is clear from Fig. 10 that 10BE has a lower thermal conductivity than that of 10BC. The main reason for this is that the MPL of 10BE has a higher amount of PTFE (50%) and a lower amount of carbon powder. Furthermore, the thermal conductivity of the PTFE, 0.25 W m^{-1} K^{-1}, is much lower than the thermal conductivity of carbon, 120 W m^{-1} K^{-1}, and 10BC has a lower amount of PTFE (30%) and a higher amount of carbon powder which increased the overall thermal conductivity of 10BC.

3.6. Effect of the temperature on the in-plane thermal conductivity of the catalyst layer

The catalyst layer is a mixture of carbon powder and platinum particles. The catalyst layers in the PEM fuel cell are in direct contact with both the membrane and the GDL layers. These five layers are compressed together to form the membrane electrode assembly (MEA).

The thermal conductivity of an in-house fabricated 10BA GDL-based MEA is measured in order to determine the thermal conductivity of the catalyst layer which is reported to be between 0.2 and 1.5 W m^{-1} K^{-1} [28,6]. The thickness of the catalyst layer was estimated to be 3×10^{-5} m, the thickness of the membrane was 1.27×10^{-4} m and the thickness of the GDL was 4×10^{-4} m. The platinum loadings was about 0.4 mg cm^{-2} which corresponds to 60% Pt/C.

The thermal conductivity of the catalyst layer was estimated by making use of the measured conductivity of the entire MEA and previously-measured conductivities for the membrane and the GDLs:

$$k_{\mathrm{MEA}} = 2(\nu_{\mathrm{GDL}} k_{\mathrm{GDL}}) + \nu_{\mathrm{mem}} k_{mem} + 2(\nu_{\mathrm{cl}} k_{\mathrm{cl}}) \quad (9)$$

where k_{MEA} is the thermal conductivity of the membrane electrode assembly. k_{GDL}, k_{cl} and k_{mem} are the thermal conductivities of GDL,

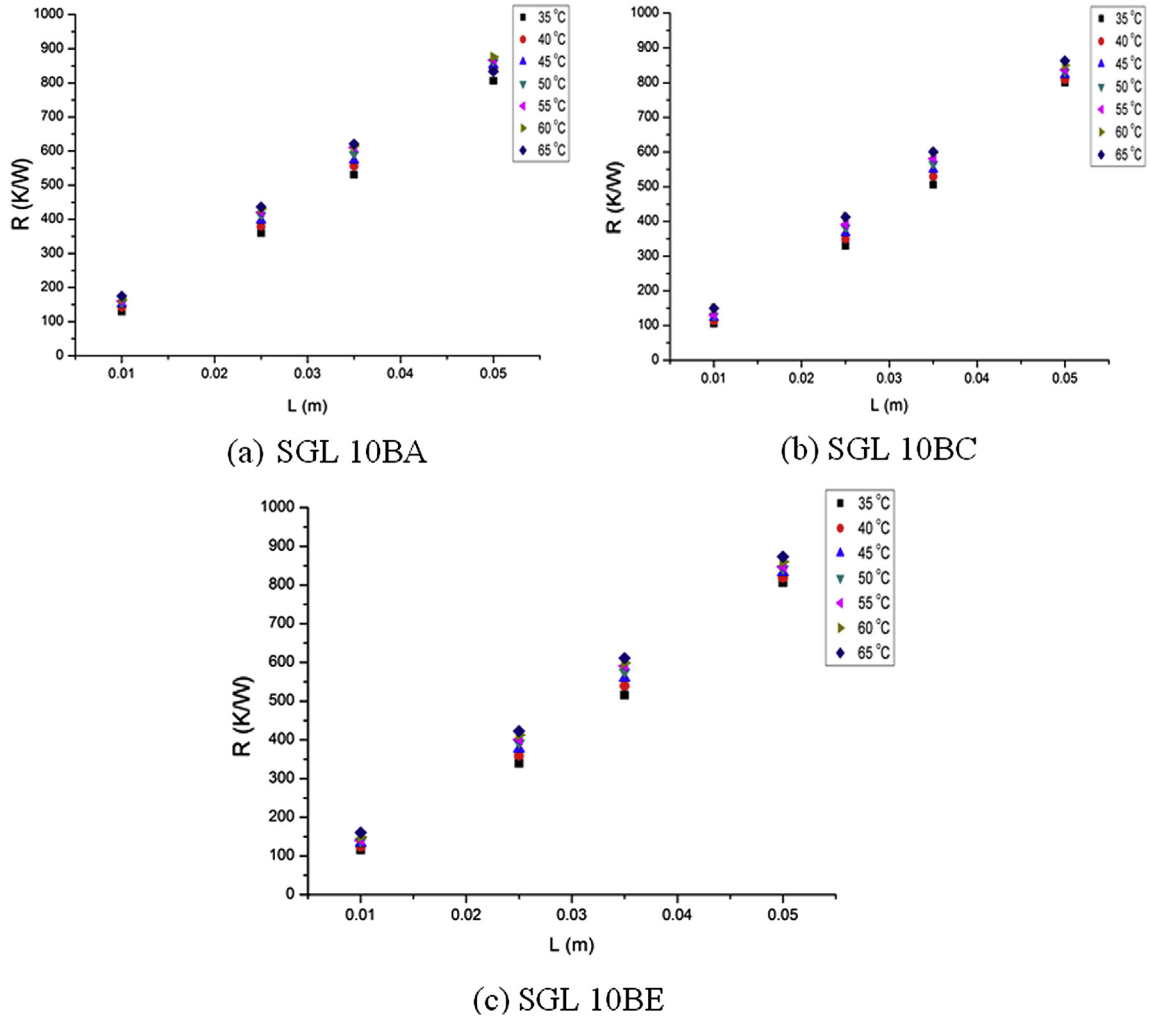

Fig. 8. Measured thermal resistance for the tested GDLs (a) SGL 10BA, (b) SGL 10BC, and (c) SGL 10BE.

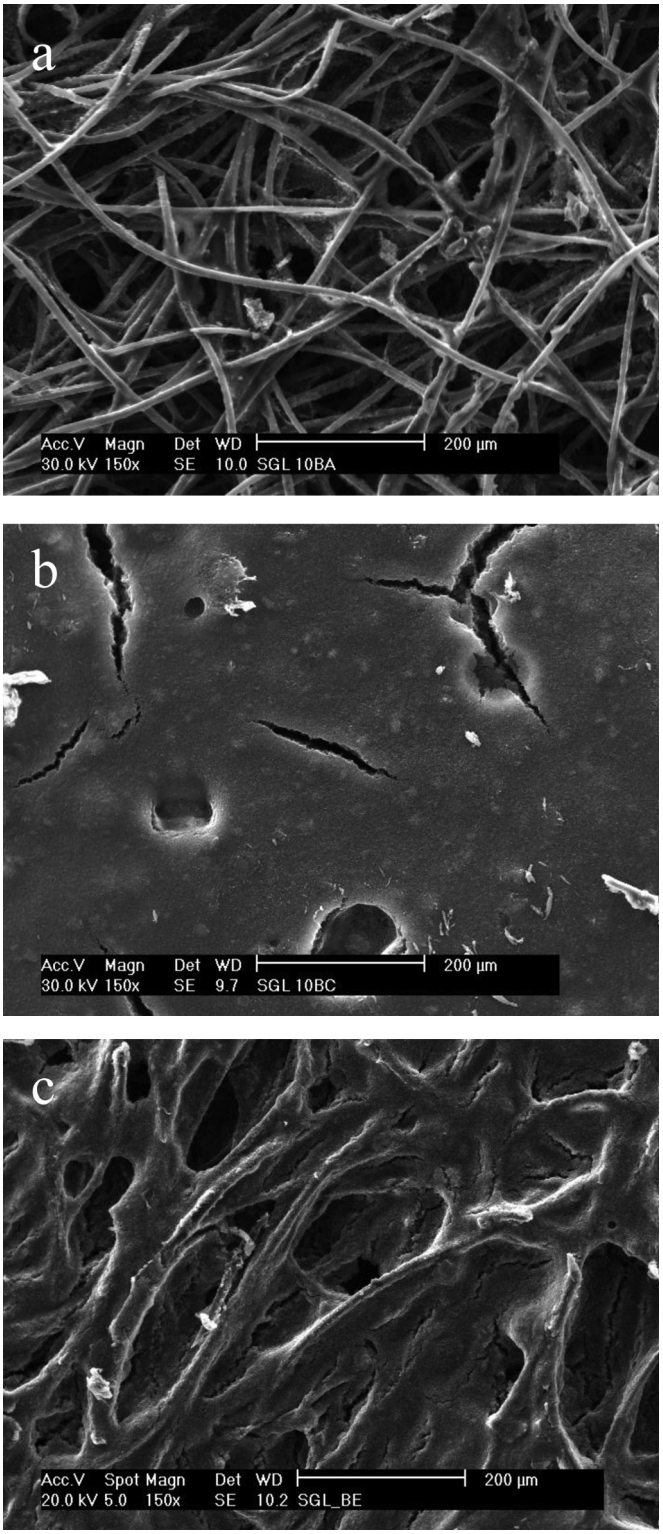

Fig. 9. SEM images for the surface of the GDLs (a) SGL 10BA, (b) SGL 10BC, and (c) SGL 10BE [27].

catalyst layer and membrane, respectively. ν_{GDL}, ν_{cl} and ν_{mem} are the volume fractions of GDL, catalyst layer and membrane, respectively [14].

Fig. 11 shows the thermal conductivity of the catalyst layer as a function of the temperature. It was observed that the thermal conductivity of the catalyst is almost independent of the

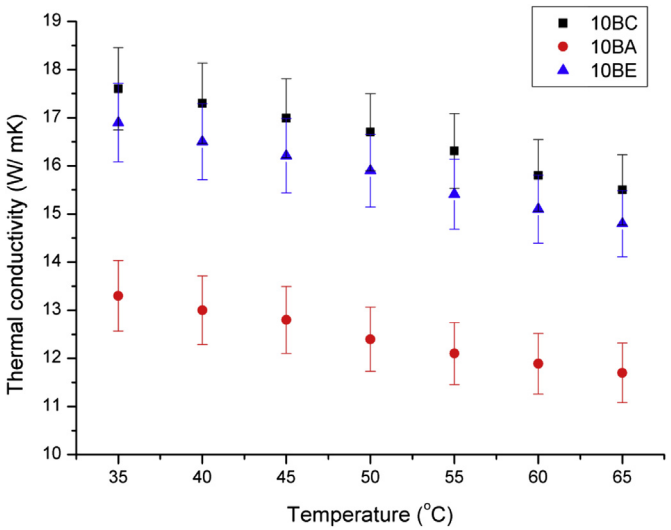

Fig. 10. Measured thermal conductivities of the investigated GDLs (10BA, 10BC and 10BE) as a function of the temperature along with the experimental error bars.

temperature and it was 0.291 ± 0.018 W m^{-1} K^{-1}. This value is in a good agreement with the reported value of the thermal conductivity of the catalyst layer by Kandelwal and Mench [6], namely 0.27 ± 0.05 W m^{-1} K^{-1}, as they used the same method by estimating the thermal conductivity of the catalyst from the thermal conductivity of the MEA and they have not taken into account the effect of the temperature on the thermal conductivity of the catalyst layer.

However, there is a big assumption here as the contact resistances between the GDL and the catalyst layer and between the membrane and the catalyst layer were ignored. Furthermore, the effect of the compression the MEA on the thermal conductivity was ignored as the thermal conductivities of the GDL and the membrane inside the MEA were assumed to be the same as those of the 'bare' GDL and membrane. Therefore, the thermal conductivity of the catalyst layer was measured again after applying the catalyst to 3 samples of 10BA GDL. The resulting platinum loadings for the catalysed samples were 0.41, 0.45 and 0.51 mg cm^{-2}. The thickness and the weight of the samples were measured both before and after

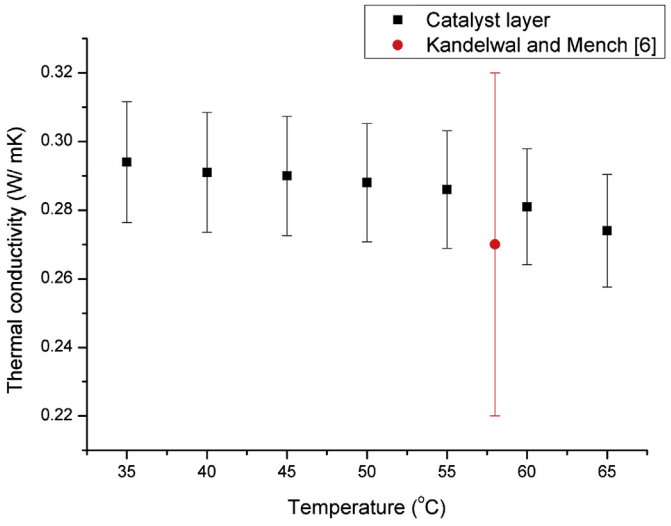

Fig. 11. Measured thermal conductivities of the catalyst in the MEA as a function of the temperature along with the experimental error bars.

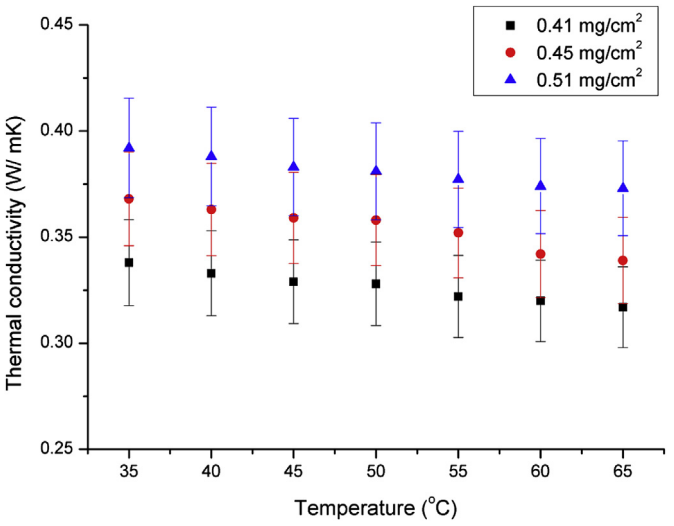

Fig. 12. Measured thermal conductivities of the catalyst layers as a function of the temperature along with the experimental error bars.

applying the catalyst in order to determine the thickness of the catalyst and calculate the volume fractions of the GDL and the catalyst. In addition, the thermal conductivities of these three GDL samples were measured before and after applying the catalyst. The thermal conductivity of the catalysed GDL can be expressed as follows:

$$k_{\text{total}} = \nu_{\text{GDL}} k_{\text{GDL}} + \nu_{\text{cl}} k_{\text{cl}} \tag{10}$$

The thermal conductivity of the catalyst is measured for these three samples in order to accurately measure the thermal conductivity of the catalyst layer and investigate the effect of Pt loadings on the thermal conductivity of the catalyst layer, with the results summarised in Fig. 12. It is clear from the figure that the thermal conductivity of the catalyst layer was higher that the reported value in Fig. 11 and it increases slightly with increasing Pt loading. This is due to the addition of platinum which has a thermal conductivity of 71.6 W m^{-1} K^{-1} in this range of temperatures [29]. Moreover, the thermal conductivity of the catalyst is found to be insensitive to the temperature. The maximum thermal conductivity of the catalyst layer with a platinum loading of 0.41 mg cm^{-2} is 0.338 ± 0.020 W m^{-1} K^{-1} when the temperature is 35 °C, and the minimum thermal conductivity of this catalyst layer is 0.317 ± 0.019 W m^{-1} K^{-1} when the temperature is 65 °C.

4. Conclusions

The parallel thermal conductance technique has been employed to measure the thermal conductivity of the GDL as a function of the temperature, fibre direction, PTFE loading and MPL coating. Also, the thermal conductivities of the membrane and the catalyst layer have been experimentally estimated. The main conclusions of these measurements are as follows:

- The thermal conductivity of the membrane decreases when the temperature increases. The thermal conductivity of the Nafion® 115 membrane was found to be 0.188 ± 0.015 W m^{-1} K^{-1} and 0.135 ± 0.011 W m^{-1} K^{-1} when the temperature was 35 °C and 65 °C, respectively.
- The in-plane thermal conductivity of the GDL decreases as the temperature increases from 35 °C to 65 °C. This decrease is due to the fact that the GDL consists of a polymeric resin and/or PTFE whose thermal conductivities decrease with increasing temperature. The in-plane thermal conductivity of the GDL increases slightly with PTFE loading. This is due to the fact that the PTFE is replacing air, which has a lower thermal conductivity than that of the PTFE. Moreover, the thermal contact resistance between the fibres reduce when adding PTFE between the fibres and this assists in the transfer of heat along the fibres, thus increasing the in-plane thermal conductivity of the GDL. The in-plane thermal conductivity of the GDL is higher when the fibres are oriented parallel to the heat flux as this provides a direct and easy way for the heat to be transferred along the fibre. It is found that the in-plane thermal conductivity of the GDL is higher in the samples which contain MPLs and this is due to the fact that the MPLs used are rich in carbon which is a highly conductive material compared to the material of the non-coated GDL. Therefore, the overall thermal conductivity of the coated GDL increases.
- The in-plane thermal conductivity of the catalyst layer was found to be insensitive to the temperature and increases with Pt loading.

The performance of the PEM fuel cell improves with increasing the thermal conductivity of the components of the MEA and this is due to better heat dissipation. Therefore, these measurements can be used to provide a basis for better designs for the PEM fuel cells and thus enhance their performance. Furthermore, these parameters could be used in PEM fuel cells models to predict a more accurate temperature distribution in the fuel cell and this will assists in the thermal management of the PEM fuel cell.

Acknowledgement

The authors would like to thank Mr Paul Crosby for his technical support in the experimental work and the first author would like to thank the Ministry of Higher Education in Saudi Arabia for the financial support.

Nomenclature

A	cross-sectional area of the sample (m^2)
I	current density magnitude (A m^{-2})
k	thermal conductivity (W m^{-1} K^{-1})
k_{air}	thermal conductivity of air (W m^{-1} K^{-1})
k_{cl}	thermal conductivity of catalyst layer (W m^{-1} K^{-1})
k_{GDL}	thermal conductivity of GDL (W m^{-1} K^{-1})
k_{MEA}	thermal conductivity of the membrane electrode assembly (W m^{-1} K^{-1})
k_{mem}	thermal conductivity of membrane (W m^{-1} K^{-1})
k_{water}	thermal conductivity of water (W m^{-1} K^{-1})
L	length (m)
Q	heat transfer (W)
R	total thermal resistance (K W^{-1})
R_{CR}	thermal contact resistance (m^2 K W^{-1})
R_s	sample thermal resistance (K W^{-1})
R_0	holder thermal resistance (K W^{-1})
RH	relative humidity
T_c	cold plate temperature (°C)
T_h	hot plate temperature (°C)
ΔT	temperature drop (K)
V	voltage (V)
ν_{air}	volume fraction of air
ν_{cl}	volume fraction of catalyst
ν_{GDL}	volume fraction of GDL
ν_{mem}	volume fraction of membrane
ν_{water}	volume fraction of water

Abbreviations

CL	catalyst layer
GDL	gas diffusion layer
MEA	membrane electrode assembly
MPL	micro porous layer
PEM	proton exchange membrane
PTC	parallel thermal conductance
PTFE	polytetrafluoroethylene

References

[1] P.J.S. Vie, S. Kjelstrup, Electrochimica Acta 49 (2004) 1069–1077.
[2] G. Maggio, V. Recupero, C. Mantegazza, Journal of Power Sources 62 (1996) 167–174.
[3] T. Berning, D.M. Lu, N. Djilali, Three-dimensional Computational Analysis of Transport Phenomena in a PEM Fuel Cell, Elsevier, 2002.
[4] M. Hamour, J.P. Garnier, J.C. Grandidier, A. Ouibrahim, S. Martermianov, International Journal of Thermophysics 32 (2011) 1025–1037.
[5] N. Zamel, x. Li, J. Shen, A. Wiegmann, J. Becker, Chemical Engineering Science 65 (2010) 3994–4006.
[6] M. Khandelwal, M. Mench, Journal of Power Sources 161 (2006) 1106–1115.
[7] O. Burheim, P.J.S. Vie, J.G. Pharoah, S. Kjelstrup, Journal of Power Sources 195 (2010) 249–256.
[8] P. Teertstra, G. Karimi, X. Li, Electrochimica Acta 56 (2011) 1670–1675.
[9] E. Sadeghi, N. Djilali, M. Bahrami, Journal of Power Sources 196 (2011) 3565–3571.
[10] G. Karimi, X. Li, P. Teertstra, Electrochimica Acta 55 (2010) 1619–1625.
[11] B.M.L. Zawilski, T. Roy, T.M. Tritt, Review of Scientific Instruments 72 (2001) 1770–1774.
[12] X. Tang, K. Aaron, J. He, T.M. Tritt, Physica Status Solidi A 205 (2008) 1152–1156.
[13] T.M. Tritt, Thermal Conductivity: Theory, Properties, and Applications, Kluwer Academic/Plenum Publishers, 2004.
[14] R.J. Moffat, Experimental Thermal and Fluid Science 1 (1988) 3–17.
[15] K.A. Mauritz, R.B. Moore, Chemical Reviews (2004) 4535–4585.
[16] M. Sahimi, Flow and Transport in Porous Media and Fractured Rock, Wiley, 2012.
[17] G. Dagan, Flow and Transport in Porous Formations, Springer-Verlag, 1989.
[18] S. Um, C.Y. Wang, K.S. Chen, Journal of the Electrochemical Society 147 (2000) 4485–4493.
[19] V. Gurau, H. Liu, S. Kakaç, AIChE Journal 44 (1998) 2410–2422.
[20] Nafion product sheet, Dupont USA.
[21] M.L.V. Ramires, C. Nieto, Y. Nagasaka, A. Nagashaima, M. Assael, W. Wakeham, Journal of Physical and Chemical Reference Data 24 (1995) 1377–1381.
[22] D.M. Price, M. Jarratt, Thermochimica Acta (2002) 231–236.
[23] N. Zamel, E. Litovsky, S. Shakhshir, X. Li, J. Kleiman, International Journal of Hydrogen Energy 36 (2011) 12618–12625.
[24] J. Blumm, M. Meyer, C. Strasser, International Journal of Thermophysics 31 (2010) 1919–1927.
[25] K. Stephan, A. Laesecke, Journal of Physical and Chemical Reference Data 14 (1985) 227–234.
[26] J. Ramousse, O. Lottin, S. Didierjean, D. Maillet, International Journal of Thermal Sciences 47 (2008) 1–6.
[27] M.S. Ismail, D.B. Inghama, L. Ma, M. Pourkashaniana, International Journal of Energy Research (2012), http://dx.doi.org/10.1002/er.2968.
[28] A. Rowe, X. Li, Journal of Power Sources 102 (2001) 82–96.
[29] R.P. Bhatta, S. Annamalai, R.K. Mohr, M. Brandys, I.L. Pegg, Review of Scientific Instruments 81 (2010) 114904–114905.